

Temperature dependence of the spin Seebeck effect in $[\text{Fe}_3\text{O}_4/\text{Pt}]_n$ multilayers

R. Ramos, T. Kikkawa, A. Anadón, I. Lucas, K. Uchida, P. A. Algarabel, L. Morellón, M. H. Aguirre, E. Saitoh, and M. R. Ibarra

Citation: *AIP Advances* **7**, 055915 (2017); doi: 10.1063/1.4974060

View online: <http://dx.doi.org/10.1063/1.4974060>

View Table of Contents: <http://aip.scitation.org/toc/adv/7/5>

Published by the [American Institute of Physics](#)

Articles you may be interested in

[Probing the temperature-dependent magnetic anisotropy and longitudinal spin Seebeck effect in \$\text{Y}_3\text{Fe}_5\text{O}_{12}\$](#)
AIP Advances **7**, 055912055912 (2017); 10.1063/1.4973948

[Magnetoelectric tuning of the inverse spin-Hall effect](#)
AIP Advances **7**, 055911055911 (2017); 10.1063/1.4973845

[Spin Seebeck effect in insulating epitaxial \$\gamma\text{-Fe}_2\text{O}_3\$ thin films](#)
AIP Advances **5**, 026103026103 (2017); 10.1063/1.4975618

[Robust spin-current injection in lateral spin valves with two-terminal \$\text{Co}_2\text{FeSi}\$ spin injectors](#)
AIP Advances **7**, 055808055808 (2016); 10.1063/1.4972852

HAVE YOU HEARD?

Employers hiring scientists and
engineers trust

PHYSICS TODAY | JOBS

www.physicstoday.org/jobs



Temperature dependence of the spin Seebeck effect in $[\text{Fe}_3\text{O}_4/\text{Pt}]_n$ multilayers

R. Ramos,^{1,2,a} T. Kikkawa,^{1,3} A. Anadón,^{4,5} I. Lucas,^{4,5} K. Uchida,^{3,6,b}
 P. A. Algarabel,^{5,7} L. Morellón,^{4,5} M. H. Aguirre,^{4,5,8} E. Saitoh,^{1,2,3,9}
 and M. R. Ibarra^{4,5,8}

¹WPI Advanced Institute for Materials Research, Tohoku University, Sendai 980-8577, Japan

²Spin Quantum Rectification Project, ERATO, Japan Science and Technology Agency, Sendai 980-8577, Japan

³Institute for Materials Research, Tohoku University, Sendai 980-8577, Japan

⁴Instituto de Nanociencia de Aragón, Universidad de Zaragoza, E-50018 Zaragoza, Spain

⁵Departamento de Física de la Materia Condensada, Universidad de Zaragoza, E-50009 Zaragoza, Spain

⁶PRESTO, Japan Science and Technology Agency, Saitama 332-0012, Japan

⁷Instituto de Ciencia de Materiales de Aragón, Universidad de Zaragoza and Consejo Superior de Investigaciones Científicas, 50009 Zaragoza, Spain

⁸Laboratorio de Microscopías Avanzadas, Universidad de Zaragoza, E-50018 Zaragoza, Spain

⁹Advanced Science Research Center, Japan Atomic Energy Agency, Tokai 319-1195, Japan

(Presented 4 November 2016; received 23 September 2016; accepted 25 October 2016; published online 11 January 2017)

We report temperature dependent measurements of the spin Seebeck effect (SSE) in multilayers formed by repeated growth of a $\text{Fe}_3\text{O}_4/\text{Pt}$ bilayer junction. The magnitude of the observed enhancement of the SSE, relative to the SSE in the single bilayer, shows a monotonic increase with decreasing the temperature. This result can be understood by an increase of the characteristic length for spin current transport in the system, in qualitative agreement with the recently observed increase in the magnon diffusion length in Fe_3O_4 at lower temperatures. Our result suggests that the thermoelectric performance of the SSE in multilayer structures can be further improved by careful choice of materials with suitable spin transport properties. © 2017 Author(s). All article content, except where otherwise noted, is licensed under a Creative Commons Attribution (CC BY) license (<http://creativecommons.org/licenses/by/4.0/>). [<http://dx.doi.org/10.1063/1.4974060>]

Thermoelectric conversion is one of the promising approaches for implementation of wasted heat energy recovery and temperature sensing technologies. Recently, a spin-based approach has been discovered: the spin Seebeck effect (SSE).¹ The SSE refers to the generation of spin currents² in a ferromagnetic material (F) upon application of a temperature gradient, the spin current is injected and electrically detected in a normal metal (N) in contact with F, where spin-orbit interaction in N transforms the spin current into an electric field, by means of the inverse spin Hall effect (ISHE),³ which can be expressed as:

$$\mathbf{E}_{\text{ISHE}} = \theta_{\text{SH}} \rho (\mathbf{J}_S \times \boldsymbol{\sigma}), \quad (1)$$

where θ_{SH} and ρ denote the spin Hall angle and electric resistivity of N, respectively. \mathbf{E}_{ISHE} , \mathbf{J}_S , and $\boldsymbol{\sigma}$ are the ISHE generated electric field, spatial direction of spin current (perpendicular to the F/N interface) and spin-polarization vector (parallel to the magnetization). A schematic diagram of the SSE is shown in Fig. 1(a), by measuring the voltage V between the ends of the N film, the SSE is electrically detected by means of the ISHE as $V_{\text{ISHE}} = E_{\text{ISHE}} L_y$.

^aramosr@imr.tohoku.ac.jp

^bPresent address: National Institute for Materials Science, Tsukuba 305-0047, Japan.

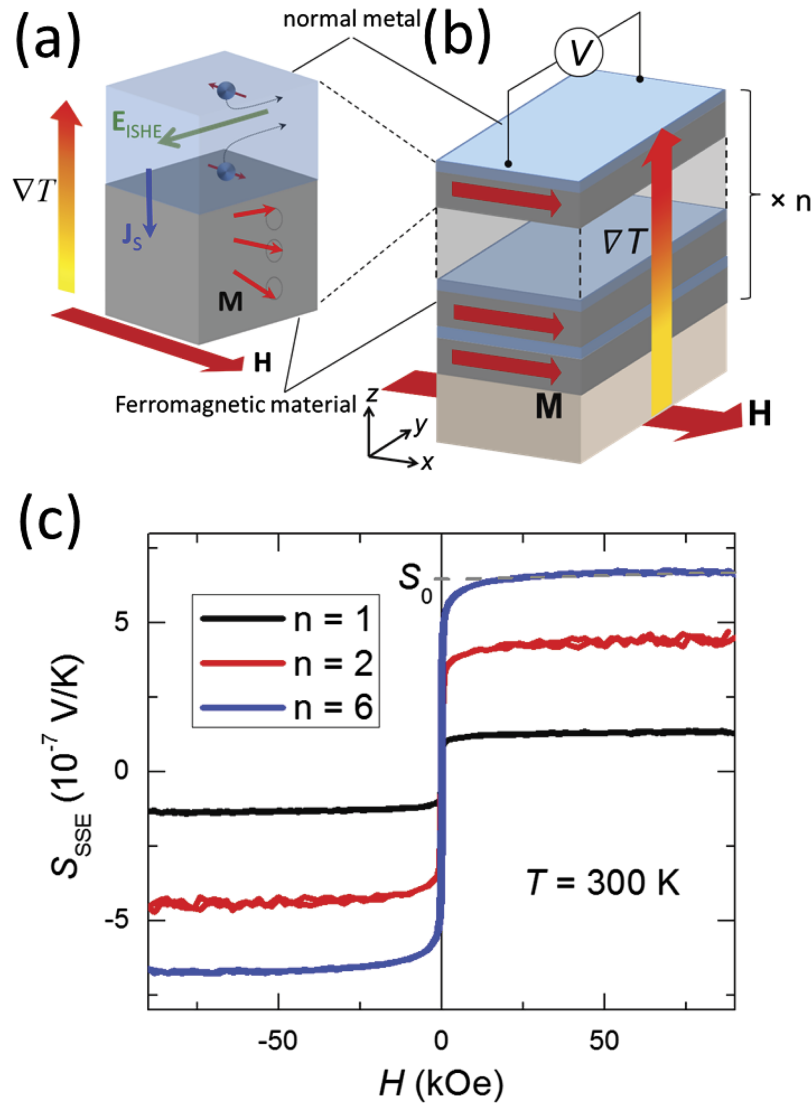


FIG. 1. (a) Schematic illustrations of the spin Seebeck effect (SSE) with the induced inverse spin Hall effect (ISHE) in a non-magnetic metal attached to a ferromagnetic material, E_{ISHE} denote the electric field generated by the ISHE. H , M , ∇T , and J_S denote the magnetic field, magnetization, temperature gradient, and spatial direction of the spin current, respectively. (b) Schematic illustration of the multilayer samples. (c) Spin Seebeck thermopower in the multilayers as a function of the applied magnetic field measured at 300 K.

The SSE has been experimentally established as a general transport phenomenon in ferromagnets and observed in a wide range of magnetic materials,^{1,4-7} triggering intensive research on the interplay between spin, charge and heat currents, which is the focus of spin caloritronics.^{8,9}

The SSE was initially explained as a result of the thermal non-equilibrium between magnons in F and conduction electrons in N, generating a spin current at the F/N interface, proportional to the effective temperature difference between magnons in F and electrons in N.¹⁰⁻¹² Recently, other theories also highlight the role of the magnon spin currents within the ferromagnet,^{13,14} which is supported by experimental reports.¹⁵⁻¹⁸

The observation of the SSE in magnetic insulators has opened the possibility to generate pure spin currents with lesser dissipation losses due to mobile charge carriers, and further expand the range of possible materials to study spin mediated thermoelectric conversion. Moreover, the experimental geometry of the SSE with the thermal and electric current paths perpendicular to each other is advantageous for the implementation of thin film and flexible thermoelectric devices.^{19,20}

Furthermore, due to the fact that the heat and electric currents have independent paths, the properties of the different materials comprising the SSE device can be optimized independently. However, there is one main disadvantage for the potential application of the SSE, this is the low magnitude of the thermoelectric output. Different possibilities are currently being explored,²¹ such as increasing the spin current detection efficiency by taking advantage of the spin Hall angle characteristics of different N materials,^{22–25} as it was shown by the implementation of spin Hall thermopiles.²⁶ However, using this approach increases the thermoelectric voltage at the expense of the extractable electrical power due to increased internal resistance of the thermopile devices.²⁷ Other approaches can be directed towards increasing the thermal spin current generation, as recently shown in spin induced thermoelectric measurements in magnetic multilayers.^{17,28–30}

Here, we have investigated the temperature dependence of the SSE in $[\text{Fe}_3\text{O}_4/\text{Pt}]_n$ multilayers. This can be related to the change of the spin transport properties with the temperature of the materials comprising the SSE system.^{15,16,31,32} Moreover, it can provide further information about the enhancement mechanism and a possible route to further improve the heat to electricity conversion efficiency of multilayer based SSE devices.

The multilayer structures were obtained by sequential growth of n number of F/N bilayer junctions, hereafter referred to as $[\text{F}/\text{N}]_n$ [see Fig. 1(b) for a schematic of the multilayer structure]. The materials used to form the basic F/N bilayer structure are magnetite ($\text{F} \equiv \text{Fe}_3\text{O}_4$), and platinum ($\text{N} \equiv \text{Pt}$). Magnetite is a ferrimagnetic oxide with high Curie temperature and predicted half-metallic nature, commonly studied in spintronics.^{33–37} Pt is used as the spin current detector, due to its relatively large spin Hall angle.^{38,39} Despite Fe_3O_4 being electrically conductive, it has been previously shown that the SSE dominates the thermoelectric response of the transversal voltage in $\text{Fe}_3\text{O}_4/\text{Pt}$ system due to the fact that the electrical conductivity of magnetite is two orders of magnitude lower than that of Pt.⁴⁰

The Fe_3O_4 films were grown on magnesium oxide, $\text{MgO}(001)$, substrates by pulsed laser deposition using a KrF excimer laser with 248 nm wavelength, 10 Hz repetition rate, and $3 \times 10^9 \text{ W}/\text{cm}^2$ irradiance in an ultrahigh-vacuum chamber (UHV). The Pt films were deposited by DC magnetron sputtering in the same UHV chamber. The films thicknesses are 34 nm for Fe_3O_4 and 17 nm for Pt. Further details on the growth can be found elsewhere.⁴¹ The film structural quality was confirmed by x-ray diffraction and transmission electron microscopy. The SSE experiments were performed using the longitudinal configuration,⁴² the sample is placed between two AlN plates with high thermal conductivity acting as heat baths. A thin layer of thermal grease is uniformly applied between the AlN plates and the sample to improve thermal contact condition. By passing an electric current to a heater attached to the top plate, a thermal gradient (∇T) is induced in the z direction. This generates a temperature difference (ΔT) between the top and bottom plates, which are stabilized at temperatures T and $T + \Delta T$, respectively. The temperature difference between the heat baths is monitored by two thermocouples connected differentially. A magnetic field is swept in the x direction while the SSE voltage in the top Pt film is measured along the y direction with a nanovoltmeter. Despite placing the electric contacts on the top Pt layer, we can consider that all the Pt layers are simultaneously connected in parallel due to the fact that the lateral dimensions of the sample are six orders of magnitude larger than the thickness of the layers, therefore the out-of-plane resistance is negligibly small compared to the in-plane resistance. The sample dimensions are $L_x = 2 \text{ mm}$, $L_y = 7 \text{ mm}$ and $L_z = 0.5 \text{ mm}$.

Figure 1(c) shows the comparative results for the magnetic field dependence of the transverse thermopower [$S_{\text{SSE}} = (V/\Delta T)(L_z/L_y)$] measured at 300 K for three samples with different number of $\text{Fe}_3\text{O}_4/\text{Pt}$ bilayers; $n = 1, 2$, and 6. The magnitude of the SSE thermopower monotonically increases with n , with a factor of 4 increase for the $[\text{Fe}_3\text{O}_4/\text{Pt}]_6$ multilayer, respect to that observed for the single $\text{Fe}_3\text{O}_4/\text{Pt}$ bilayer junction. The observed enhancement cannot be explained by conventional spin current injection at the F/N interface. Even when considering injection from both top and bottom surfaces of the Pt layers, only a maximum increase of twice the bilayer voltage can be explained. We have previously proposed a mechanism for the enhancement of the SSE in the $[\text{Fe}_3\text{O}_4/\text{Pt}]_n$ multilayers.¹⁷ The model basically considers the boundary conditions for spin currents flowing parallel to the thickness direction. The spin current must vanish at the top and bottom surfaces of the multilayer structure, while the spin current at the F/N (N/F) interfaces of the multilayer is assumed to

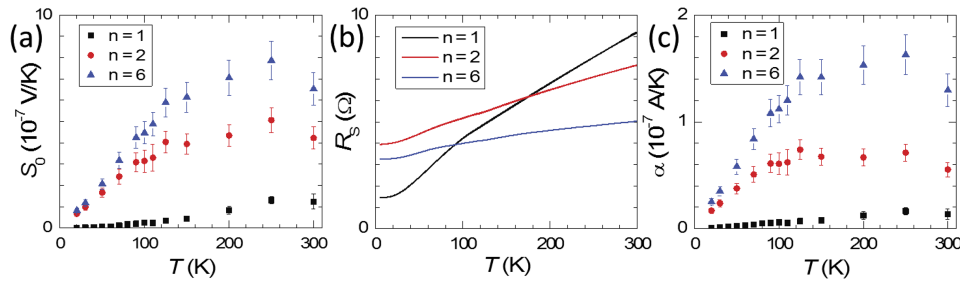


FIG. 2. Temperature dependence of the (a) SSE coefficient, (b) SSE sample sheet resistance, R_S and (c) estimated thermoelectric current $\alpha = S_0/R_S$ for different bilayer numbers, n .

be continuous.^{13,14} As a consequence, an increase of the spin current magnitude is expected with maximum values at the middle layers of the multilayer. The overall thickness dependence of the spin current within the multilayer is characterized by a length scale (ξ) defined as $\xi = \sqrt{\frac{G_S}{2} \frac{t_F + t_N}{\sqrt{[(t_F/\Lambda) + (t_N/\lambda)]}}}$, where t_F (t_N) and Λ (λ) are the thickness and magnon (conduction-electron) spin diffusion lengths in the ferromagnet (normal metal), respectively. G_S is a dimensionless spin conductance for the F/N interface.¹⁷ The SSE enhancement in multilayers can be determined by this length scale ξ , therefore by studying the temperature dependence of the enhancement, we can possibly relate it to the variation of the spin transport properties in the $\text{Fe}_3\text{O}_4/\text{Pt}$ system.

Figure 2(a) shows the measured temperature dependence of the SSE in multilayers as a function of the number of bilayers, with $n = 1, 2$, and 6 . The data represents the magnitude of the zero field intercept (S_0), obtained from extrapolating the SSE data at high magnetic fields to the zero field value [as shown in Fig. 1(c)]. The magnitude of the SSE thermopower shows a gradual decrease as the temperature is reduced. The value of the measured voltage can be influenced by the internal resistance of the sample, therefore we have measured the temperature dependence of the resistance in order to compare the data between different samples. Figure 2(b) shows the temperature dependence of the sheet resistance, $R_S = RL_x/L_y$ measured using 4-probe method. It can be clearly observed that all samples present metallic behaviour with a monotonic resistance decrease as the temperature is reduced. It is interesting to note that the decrease is less pronounced for the sample with larger number of bilayers ($n=6$), this difference in the temperature dependence of resistance between the samples can be possibly attributed to a contribution from a non-negligible out-of-plane resistance of the magnetite thin films, which adds up as the number of layers increases. In order to remove the contribution from the resistance on the observed voltage enhancement and compare the data between the different samples, we consider the SSE thermopower normalized by the sheet resistance of the sample, given by the quantity $\alpha = S_0/R_S$. This quantity is equivalent to the thermoelectric current generated in the sample. Figure 2(c) shows the obtained data, it can be seen that the behaviour is similar to that observed for the SSE thermopower, with the magnitude of the thermoelectric current gradually decreasing as the temperature is reduced. It is interesting to note that the temperature dependence of α (and S_0) shows a less pronounced decrease in the case of the multilayer samples. Usually, two factors play a role in the temperature dependence of the SSE: one is the reduction of the magnon population at low temperatures, responsible for the decreasing SSE at low temperatures, and the other is due to the increased spin current lifetime which increases the SSE magnitude as the temperature is reduced.^{14,15,43,44} The weaker temperature dependence in the case of the SSE in multilayers can possibly be understood by the increase of the length scale for spin current propagation ξ , resulting in a larger contribution from the later factor and therefore a less pronounced reduction of the SSE compared to the single bilayer. Therefore, we will focus on the multilayer length scale ξ to discuss the temperature dependence of the SSE enhancement in multilayers.

Now, we proceed to compare the temperature dependence of the SSE enhancement in multilayers, in order to do so, we define an enhancement factor as the ratio of the thermoelectric current between the multilayers and the single bilayer [enhancement factor $\equiv \alpha(n)/\alpha(1)$], as shown in Fig. 3. It can be

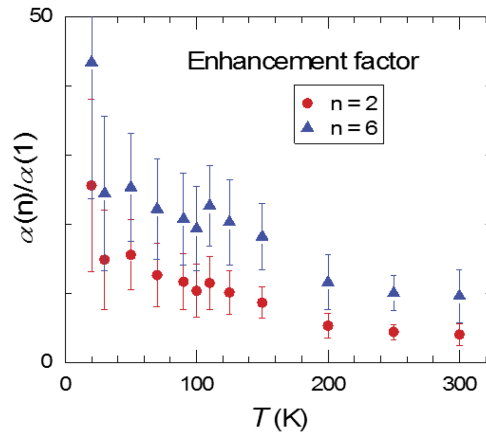


FIG. 3. Temperature dependence of the estimated enhancement factor [$\alpha(n)/\alpha(1)$].

clearly seen that the SSE enhancement monotonically increases as the temperature of the system is reduced. If we consider the expression for ξ , for a constant thickness of the films comprising the basic $\text{Fe}_3\text{O}_4/\text{Pt}$ junction, we can expect an enhancement of ξ for increasing values of the magnon (Λ) and conduction-electron (λ) spin diffusion lengths in Fe_3O_4 and Pt respectively. Previous experiments on the dependence of the SSE on the ferromagnet thickness report an increasing magnon diffusion length as the temperature of the system is reduced.^{15,16,31} The magnon diffusion length for magnetite thin films has been shown to increase at lower temperatures, showing a magnitude 2-3 times larger at 70 K than at room temperature. For comparison we will consider the multilayer enhancement increase between the same temperatures. Figure 3 shows that the observed SSE enhancement in $[\text{Fe}_3\text{O}_4/\text{Pt}]_n$ multilayers increases by a factor of two between 300 K and 70 K.

Using the expression for ξ described above, the observed enhancement can be understood in terms of an increase of the magnon and spin diffusion lengths of Fe_3O_4 ³¹ and Pt, respectively. If we consider a value of $\lambda = 3$ nm at 300 K,⁴⁵ and assume that the G_S factor is temperature independent, we can explain the increase in the enhancement factor observed at 70 K by a value of $\lambda = 13$ nm. Previous reports of the spin diffusion length in Pt, measured using non-local spin valves,³² have also shown an increasing tendency of the magnitude at lower temperatures, however the reported increase is much lower, with only a 70% increase. The authors argue that the low values of the spin diffusion length at low temperatures can be possibly attributed to the higher resistivity of their Pt films in comparison to other studies.⁴⁶ In a recent report by the same group, they further show that the Pt spin diffusion length is strongly dependent on the sample quality, presenting a linear dependence with the electrical conductivity of the films.⁴⁷ This can possibly explain the larger increase in λ obtained from our estimation, since the Pt films used in our study are highly oriented crystalline films.²⁷ For instance, the electrical conductivity of the Pt film in the single bilayer increases by more than 3 times between 300 K and 70 K, which is in agreement with our estimation. However, we should bear in mind that the expression of ξ is an approximation obtained under the condition of $t_F/\Lambda, t_N/\lambda \ll 1$, which is not exactly met in our experiments. Therefore, the expression of ξ should be used only for qualitative discussion.

In summary, we have performed temperature dependent measurements of the SSE in multilayer structures based on $\text{Fe}_3\text{O}_4/\text{Pt}$ junction systems. While the magnitude of the SSE gradually decreases at low temperatures, the observed enhancement, defined as the ratio of extractable thermoelectric current between multilayers and single bilayers, shows a monotonic increase. This enhancement can be qualitatively understood as a result of an increase of the characteristic lengths for spin transport of the layers forming the multilayer structure. Our result suggests that the SSE in multilayers can be possibly further enhanced by selection of materials with larger characteristic lengths for spin transport.

This work was supported by the Spanish Ministry of Science (through projects MAT2014-51982-C2-R, including FEDER funding), the Aragón Regional Government (project E26),

Thermo-spintronic Marie-Curie CIG (Grant Agreement No. 304043), JST-PRESTO “Phase Interfaces for Highly Efficient Energy Utilization” from JST, Japan, Grant-in-Aid for Scientific Research on Innovative Areas “Nano Spin Conversion Science” (26103005), Grant-in-Aid for Scientific Research (A) (15H02012) from MEXT, Japan, NEC Corporation, and The Noguchi Institute. T.K. is supported by JSPS through a research fellowship for young scientists (15J08026).

- ¹ K. Uchida, S. Takahashi, K. Harii, J. Ieda, W. Koshibae, K. Ando, S. Maekawa, and E. Saitoh, *Nature* **455**, 778 (2008).
- ² S. Maekawa, H. Adachi, K. Uchida, J. Ieda, and E. Saitoh, *J. Phys. Soc. Jpn.* **82**, 102002 (2013).
- ³ E. Saitoh, M. Ueda, H. Miyajima, and G. Tatara, *Appl. Phys. Lett.* **88**, 182509 (2006).
- ⁴ C. M. Jaworski, J. Yang, S. Mack, D. D. Awschalom, J. P. Heremans, and R. C. Myers, *Nat. Mater.* **9**, 898 (2010).
- ⁵ K. Uchida, J. Xiao, H. Adachi, J. Ohe, S. Takahashi, J. Ieda, T. Ota, Y. Kajiwara, H. Umezawa, H. Kawai *et al.*, *Nat. Mater.* **9**, 894 (2010).
- ⁶ D. Meier, T. Kuschel, L. Shen, A. Gupta, T. Kikkawa, K. Uchida, E. Saitoh, J.-M. Schmalhorst, and G. Reiss, *Phys. Rev. B* **87**, 054421 (2013).
- ⁷ T. Niizeki, T. Kikkawa, K. Uchida, M. Oka, K. Z. Suzuki, H. Yanagihara, E. Kita, and E. Saitoh, *AIP Adv.* **5**, 053603 (2015).
- ⁸ G. E. W. Bauer, E. Saitoh, and B. J. van Wees, *Nat. Mater.* **11**, 391 (2012).
- ⁹ S. R. Boona, R. C. Myers, and J. P. Heremans, *Energy Environ. Sci.* **7**, 885 (2014).
- ¹⁰ J. Xiao, G. E. W. Bauer, K. Uchida, E. Saitoh, and S. Maekawa, *Phys. Rev. B* **81**, 214418 (2010).
- ¹¹ H. Adachi, J.-i. Ohe, S. Takahashi, and S. Maekawa, *Phys. Rev. B* **83**, 094410 (2011).
- ¹² H. Adachi, K. Uchida, E. Saitoh, and S. Maekawa, *Rep. Prog. Phys.* **76**, 036501 (2013).
- ¹³ S. S.-L. Zhang and S. Zhang, *Phys. Rev. B* **86**, 214424 (2012).
- ¹⁴ S. M. Rezende, R. L. Rodríguez-Suárez, R. O. Cunha, A. R. Rodrigues, F. L. A. Machado, G. A. Fonseca Guerra, J. C. Lopez Ortiz, and A. Azevedo, *Phys. Rev. B* **89**, 014416 (2014).
- ¹⁵ T. Kikkawa, K. Uchida, S. Daimon, Z. Qiu, Y. Shiomi, and E. Saitoh, *Phys. Rev. B* **92**, 064413 (2015).
- ¹⁶ A. Kehlberger, U. Ritzmann, D. Hinze, E.-J. Guo, J. Cramer, G. Jakob, M. C. Onbasli, D. H. Kim, C. A. Ross, M. B. Jungfleisch *et al.*, *Phys. Rev. Lett.* **115**, 096602 (2015).
- ¹⁷ R. Ramos, T. Kikkawa, M. H. Aguirre, I. Lucas, A. Anadón, T. Oyake, K. Uchida, and H. Adachi, J. Shiomi, P. Algarabel *et al.*, *Phys. Rev. B* **92**, 220407(R) (2015).
- ¹⁸ H. Jin, S. R. Boona, Z. Yang, R. C. Myers, and J. P. Heremans, *Phys. Rev. B* **92**, 054436 (2015).
- ¹⁹ A. Kirihara, K. Uchida, Y. Kajiwara, M. Ishida, Y. Nakamura, T. Manako, E. Saitoh, and S. Yorozu, *Nat. Mater.* **11**, 686 (2012).
- ²⁰ A. Kirihara, K. Kondo, M. Ishida, K. Ihara, Y. Iwasaki, A. Matsuba, K. Uchida, E. Saitoh, N. Yamamoto, and T. Murakami, *Sci. Rep.* **6**, 23114 (2016).
- ²¹ K. Uchida, H. Adachi, T. Kikkawa, A. Kirihara, M. Ishida, S. Yorozu, S. Maekawa, and E. Saitoh, *Proc. IEEE* **104**, 1946 (2016); *ibid.* **104**, 1499.
- ²² L. Liu, C.-F. Pai, Y. Li, H. W. Tseng, D. C. Ralph, and R. A. Buhrman, *Science* **336**, 555 (2012).
- ²³ C.-F. Pai, L. Liu, Y. Li, H. W. Tseng, D. C. Ralph, and R. A. Buhrman, *Appl. Phys. Lett.* **101**, 122404 (2012).
- ²⁴ Y. Niimi, Y. Kawanishi, D. H. Wei, C. Deranlot, H. X. Yang, M. Chshiev, T. Valet, A. Fert, and Y. Otani, *Phys. Rev. Lett.* **109**, 156602 (2012).
- ²⁵ P. Laczkowski, J.-C. Rojas-Sánchez, W. Savero-Torres, H. Jaffrès, N. Reyren, C. Deranlot, L. Notin, C. Beigné, A. Marty, J.-P. Attané, *et al.*, *Appl. Phys. Lett.* **104**, 142403 (2014).
- ²⁶ K. Uchida, T. Nonaka, T. Yoshino, T. Kikkawa, D. Kikuchi, and E. Saitoh, *Appl. Phys. Express* **5**, 093001 (2012).
- ²⁷ R. Ramos, A. Anadón, I. Lucas, K. Uchida, P. A. Algarabel, L. Morellón, M. H. Aguirre, E. Saitoh, and M. R. Ibarra, *APL Mater.* **4**, 104802 (2016).
- ²⁸ K.-D. Lee, D.-J. Kim, H. Yeon Lee, S.-H. Kim, J.-H. Lee, K.-M. Lee, J.-R. Jeong, K.-S. Lee, H.-S. Song, J.-W. Sohn *et al.*, *Sci. Rep.* **5**, 10249 (2015).
- ²⁹ K. Uchida, T. Kikkawa, T. Seki, T. Oyake, J. Shiomi, Z. Qiu, K. Takanashi, and E. Saitoh, *Phys. Rev. B* **92**, 094414 (2015).
- ³⁰ Y. Shiomi, Y. Handa, T. Kikkawa, and E. Saitoh, *Appl. Phys. Lett.* **106**, 232403 (2015).
- ³¹ A. Anadón, R. Ramos, I. Lucas, P. A. Algarabel, L. Morellón, M. R. Ibarra, and M. H. Aguirre, *Appl. Phys. Lett.* **109**, 012404 (2016).
- ³² M. Isasa, E. Villamor, L. E. Hueso, M. Gradhand, and F. Casanova, *Phys. Rev. B* **91**, 024402 (2014).
- ³³ I. Žutić and S. Das Sarma, *Rev. Mod. Phys.* **76**, 323 (2004).
- ³⁴ R. Ramos, S. K. Arora, and I. V. Shvets, *Phys. Rev. B* **78**, 214402 (2008).
- ³⁵ R. Ramos, M. H. Aguirre, A. Anadón, J. Blasco, I. Lucas, K. Uchida, P. A. Algarabel, L. Morellón, E. Saitoh, and M. R. Ibarra, *Physical Review B* **90**, 054422 (2014).
- ³⁶ H.-C. Wu, M. Abid, B. S. Chun, R. Ramos, O. N. Mryasov, and I. V. Shvets, *Nano Letters* **10**, 1132 (2010).
- ³⁷ H.-C. Wu, R. Ramos, R. G. S. Sofin, Z.-M. Liao, M. Abid, and I. V. Shvets, *Appl. Phys. Lett.* **101**, 052402 (2012).
- ³⁸ A. Hoffmann, *IEEE Trans. Magn.* **49**, 5172 (2013).
- ³⁹ J. Sinova, S. O. Valenzuela, J. Wunderlich, C. H. Back, and T. Jungwirth, *Rev. Mod. Phys.* **87**, 1213 (2015).
- ⁴⁰ R. Ramos, T. Kikkawa, K. Uchida, H. Adachi, I. Lucas, M. H. Aguirre, P. Algarabel, L. Morellón, S. Maekawa, E. Saitoh *et al.*, *Appl. Phys. Lett.* **102**, 072413 (2013).
- ⁴¹ J. Orna, P. A. Algarabel, L. Morellón, J. A. Pardo, J. M. de Teresa, R. López Antón, F. Bartolomé, L. M. García, J. Bartolomé, J. C. Cezar *et al.*, *Phys. Rev. B* **81**, 144420 (2010).
- ⁴² K. Uchida, H. Adachi, T. Ota, H. Nakayama, S. Maekawa, and E. Saitoh, *Appl. Phys. Lett.* **97**, 172505 (2010).
- ⁴³ S. Rezende, R. Rodríguez-Suárez, R. Cunha, J. López Ortiz, and A. Azevedo, *J. Magn. Magn. Mater.* **400**, 171 (2016).

- ⁴⁴ E.-j. Guo, J. Cramer, A. Kehlberger, C. A. Ferguson, D. A. Maclaren, G. Jakob, and M. Kläui, *Phys. Rev. X* **6**, 031012 (2016).
- ⁴⁵ V. Castel, N. Vlietstra, J. Ben Youssef, and B. J. van Wees, *Appl. Phys. Lett.* **101**, 132414 (2012).
- ⁴⁶ M. Morota, Y. Niimi, K. Ohnishi, D. H. Wei, T. Tanaka, H. Kontani, T. Kimura, and Y. Otani, *Phys. Rev. B* **83**, 174405 (2011).
- ⁴⁷ E. Sagasta, Y. Omori, M. Isasa, M. Gradhand, L. E. Hueso, Y. Niimi, Y. Otani, and F. Casanova, *Phys. Rev. B* **94**, 060412(R) (2016).